On Vorticity Dynamics in Turbulent Wake behind Circular Cylinder

Václav Uruba[1,2,*], and *Pavel* Procházka[2]

[1]Department of Power System Engineering, Faculty of Mechanical Engineering, University of West Bohemia, Universitní 8, 306 14 Plzeň, Czech Republic
[2]Department of Fluid Dynamics, Institute of Thermomechanics of the Czech Academy of Sciences, Dolejškova 5, 182 00 Praha, Czech Republic

Abstract. The circular cylinder turbulent wake is studied experimentally using Particle Image Velocimetry (PIV) method. The vorticity component parallel to the cylinder axis is evaluated from measured velocity field. Dynamics of the vorticity field is analysed using the Oscillation Pattern Decomposition (OPD) method. The 3 dominant modes corresponding to the 1st, 2nd and 3rd harmonics of Strouhal frequency are detected and presented. The corresponding topologies are characterized by waves of vortical systems. The results are similar to the dynamics of velocity field, however the procedure is much easier to implement, as only half number of degrees of freedom are active.

Keywords: *cylinder; wake; turbulence; vorticity; dynamics*

1 Introduction

Circular cylinder in cross-flow is a canonical case representing flow around a bluff-body. This problem is addressed in many studies of all kinds, experimental, theoretical and numerical studies could be find in literature published in last decades and even much earlier.

It is known, that for Reynolds numbers higher than about 44 the Kármán-Bénárd vortex street is generated in the wake. The two dimensionless parameters characterize the wake dynamics. The Reynolds number *Re* is the dimensionless velocity and the Strouhal number *Sr* is the dimensionless frequency:

$$Re = \frac{U \cdot D}{\nu}, \quad Sr = \frac{f \cdot D}{U}, \tag{1}$$

where U is the incoming flow velocity, D is the cylinder diameter, ν is the kinematic viscosity of the fluid and f is the shedding frequency of vortices in the wake.

In literature, extensive information resources could be found, starting from dawn of fluid mechanics until now. The first systematic work by von Kármán [1] followed by overview paper by Roshko [2], and Williamson [3] to mention the most cited. Interest of researches is not changing a lot during the time, however the technical means applied in the research, involving both experimental approach and mathematical modelling, have developed

* Corresponding author: uruba@it.cas.cz

substantially. Recently, we have appropriate means available for addressing even the most complex aspects of the phenomenon.

The flow dynamics in the wake represented by the Kármán vortex street has been simplified very often to a single-frequency, periodical process characterized by the Strouhal frequency. In reality, this approach could be accepted for the fully laminar case when the Reynolds number value is very low, bellow 150. For higher *Re*, the wake undergoes laminar-turbulent transition and the wake is characterized rather by a broad-band process with random component and it becomes fully 3D topology, see e.g. [4, 5]. The advanced methods for turbulent spectra from spatial data have been developed recently, see e.g. [6].

In the presented paper we will show the analysis of vorticity in the cylinder wake. The study uses the velocity data analysed directly in preceding studies [7, 8].

2 Experiment and data treatment

The experimental setup, used instrumentation and data analysis methods are to be presented in this chapter.

2.1 Experimental setup

The experiments were carried out in the IT ASCR Prague, a cylinder is placed in closed test section of the wind tunnel with the test section cross section 250 x 250 mm^2. The air flow in the test section was of a good quality, velocity departures were within 1 % of the set velocity across the test-section (outside boundary layers) and the intensity of turbulence was below 0.2 %.

In Fig. 1 there is the schematic view on the cylinder in the flow perpendicular to the cylinder axis. The green plane, parallel to the flow and perpendicular to the cylinder axis, represents the Plane of Measurement (PoM), (*xy*), in which the velocity measurement take place.

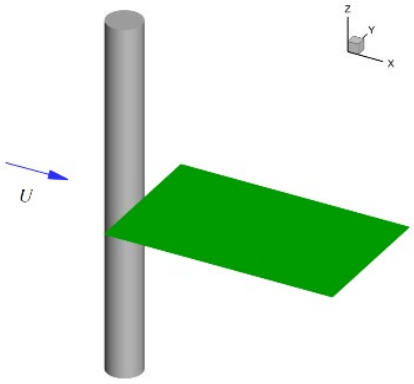

Fig. 1. Experimental setup with Plane of Measurement.

Length of the cylinder was 250 mm, diameter 15 mm, thus aspect ratio was more than 16. The flow velocity was set to 5 m/s resulting in the Reynolds number of about 4 815. The Strouhal number is expected to be around 0.21, corresponding Strouhal frequency was about 71 Hz, see [7].

2.2 Instrumentation

The Particle Image Velocimetry (PIV) technique has been applied in the PoM, see Figure 1.

The velocity vector field was measured using Particle Image Velocimetry (PIV) method. The measurement apparatus consists of laser and CMOS camera by Dantec company. The laser is New Wave Pegasus, Nd:YLF double head with wavelength of 527 nm, maximal frequency 10 kHz, shot energy is 10 mJ (for 1 kHz) and corresponding power is 10 W per one head. The camera Phantom V611 with resolution of 1 280 x 800 pixels is able to acquire double snaps with frequency up to 3000 Hz (full resolution) and it uses internal memory 8 GB. The data were acquired and post-processed in Dynamic Studio and Matlab software.

The PIV measurement was performed in the plane perpendicular to the cylinder axis and parallel to the flow direction (*xy*). The evaluated velocity fields consisting of 159 x 99 vectors were acquired in two different regimes. The data was acquired with frequency 2 kHz, the record contained 4 000 double-snapshots representing 2 s in real time.

More detailed description of the experimental setup could be found in [7, 8].

2.3 Data interpretation

The PIV method acquires instantaneous velocity field, 2 components in each measuring point. In the presented paper we will work with vorticity field, which was evaluated from the velocity field.

Vorticity $\boldsymbol{\omega}$ is a vector, mathematically it is the curl of the velocity $\mathbf{u}$:

$$\boldsymbol{\omega} = \nabla \times \mathbf{u} \,. \tag{2}$$

The physical interpretation of the vorticity is the local spin of a fluid particle. It generates vorticity rather than the rigid body rotation of a fluid mass, in which particles do not move relative to each other. It could be interpreted as twice the rotation rate of fluid particles. The vorticity is used to detect *vortices* very often, however the nonzero vorticity indicates presence of *shear* regions, which are natural part of any vortex, but not limited to them.

Essential feature of vorticity is its invariance to Galilean transform. Any linear transformation of a velocity field could change its topology as for the vortices presence, changing them into waves, however the vorticity field remains unchanged.

In our experiment, we acquired the in-plane velocity components u and v in the PoM (*xy*). Thus, we could evaluate the single vorticity component ω_z perpendicular to the PoM. For simplicity, we will refer to this scalar quantity as ω hereinafter:

$$\omega = \frac{\partial v}{\partial x} - \frac{\partial u}{\partial y} \,. \tag{3}$$

So, from the acquired velocity vector field $\mathbf{u} = [u; v]$ we obtained the scalar field ω with half number of variables.

2.4 Data analysis

The vorticity field is subjected to dynamical analysis, the spatial aspects of dynamical behaviour are to be shown next. The topology of typical structures in terms of fluctuation velocity fields are to be presented.

The Oscillation Pattern Decomposition (OPD) method is applied. The OPD method provides series of OPD modes. Each OPD mode is characterized by its topology in complex form (consisting of real and imaginary parts), frequency *f* and attenuation of the pseudo-periodic (oscillating) behavior. Attenuation or amplitude decay is described by so called e-folding time τ_e representing the mean time period of the mode amplitude decay by factor “e”.

The other decay characteristics is the dimensionless "periodicity" p which expresses the e-folding time in multiples of periods of the corresponding OPD mode defined by its frequency:

$$p = \tau_e \times f \ . \tag{4}$$

The periodicity value could be considered as a measure of "relevance" of a given OPD mode, the higher p, the higher relevance. The frequency will be represented in dimensionless form as Strouhal number Sr, see (2).

More details on the OPD method could be found in [9, 10].

3 Results

The results are to be presented in dimensionless form, coordinates are given in multiples of the cylinder diameter D.

3.1 Statistics

The time series of vorticity fields were subjected to a standard statistical analysis.

In Fig. 2 distributions of mean vorticity field (a) and standard deviations (b) are shown, respectively

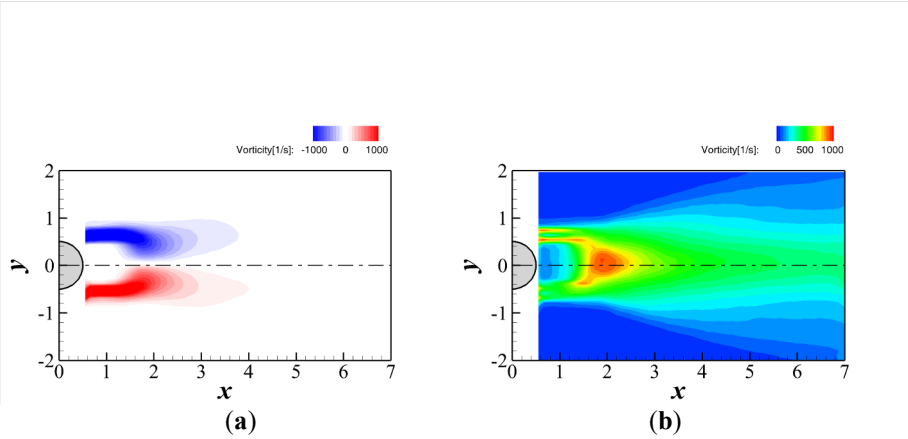

Fig. 2. Distributions of mean vorticity field (**a**) and standard deviations (**b**), respectively.

The two regions of concentrated vorticity in the near wake up-to distance 4 cylinder's diameters downstream are detected. The vorticity distribution is symmetrical around the axis x, although the vorticity sign is negative in the upper half-plane and positive in the lower half-plane. The standard deviation distribution locates well the wake border, the maximum is on the axis x in the position 2 D. the topology is symmetrical around the x-axis.

3.2 Dynamics

Dynamical analysis of the vorticity field was carried out using the OPD method. The velocity field analysis was presented in [7].

In Fig. 3 the spectrum of the dynamical analysis of velocity (a) and vorticity (b) fields are shown in Sr-p plain. The Sr_1, Sr_2 and Sr_3 represent the 1st, 2nd and 3rd harmonics of the Strouhal frequency, respectively.

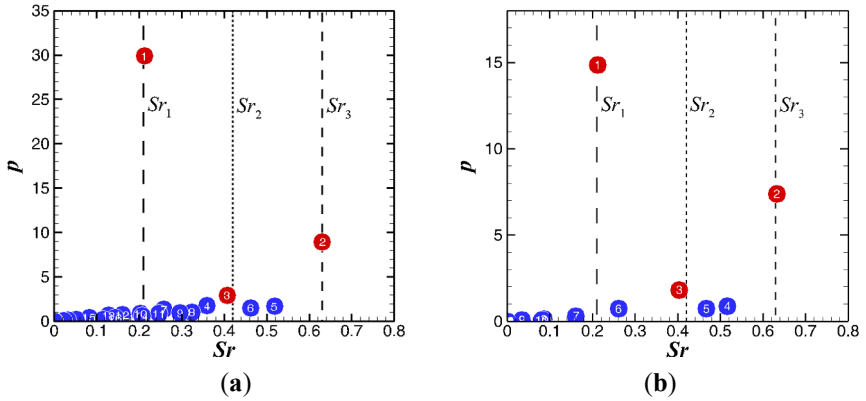

Fig. 3. OPD spectrum, velocity (**a**), vorticity (**b**).

The spectra are almost identical, however the velocity spectrum contains more high-order modes and the values of the periodicity is approximately twice as high comparing to the vorticity case. This means that the structures looks more distinct in the velocity field than in vorticity field. However in both cases we recognize the most relevant 3 OPD modes.

The most relevant OPD mode 1 is characterized by the Strouhal number $Sr_1 = 0.21$, as expected. The second mode OPD 2 corresponds to the Strouhal number $Sr_2 = 0.42$ and the second mode OPD 2 corresponds to the Strouhal number $Sr_3 = 0.63$. The OPD 3 periodicity is well above 1, thus periodical, the higher modes (4, …) have too small p indicating decaying character.

In Fig. 4 the real and imaginary parts of the OPD 1 mode topologies are shown. Please note that the vorticity values of OPD modes are normalized and thus dimensionless.

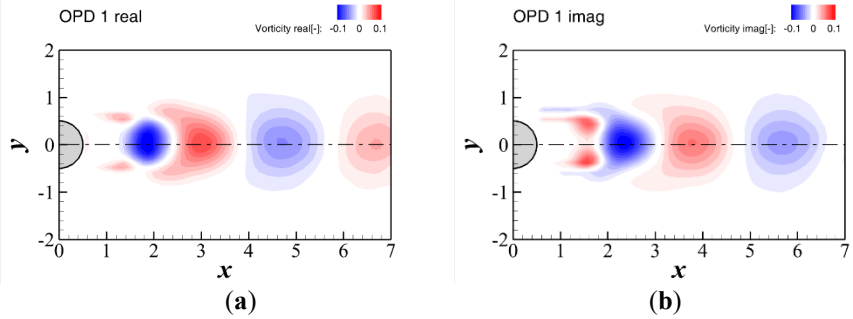

Fig. 4. OPD mode 1 topology, real (**a**) and imaginary (**b**) parts, respectively.

The real part represents 0 phase angle situation, imaginary part is the situation in $\pi/2$ phase angle (or ¼ of period, if you like), follows negative real part in π phase and negative imaginary part for phase $3\pi/2$. This cycle is repeated, the phase 2π is identical to 0 phase angle.

We could identify the vortices row with centres on the x-axis and with alternative orientations, negative and positive. In particular in the real mode topology we could recognize the negative vorticity (i.e. vortices) located in positions $x = 1.86$ and 4.71 and

positive vorticity in positions 3.02 and 6.67. In imaginary part, the vortices locations are negative in positions 2.32 and 5.66 and positive in position 3.75.

The OPD mode 1 represents the wave of vortices with alternative orientations moving downstream with velocity about 0.7U, accelerating along the axis x and getting weaker. This is exactly expected as topology of the Kármán-Bénárd vortex street.

The OPD modes 2 and 3 are again periodical with a row of vortices, real and imaginary parts are shifted in space in the same way as for the OPD 1. We will present the real parts of those OPD modes. Topologies of the OPD 2 and 3 are in Fig. 5.

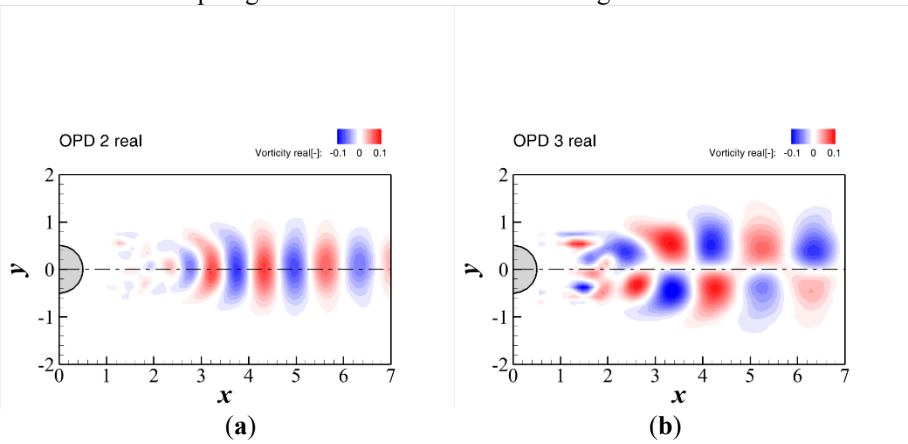

Fig. 5. OPD 2 (**a**) and 3 (**b**) topologies, real parts.

The OPD mode 2 topology in Fig. 5a is similar to the OPD 1, however the vortices spacing in x direction is about 1/3. The vortices are squeezed, as spanwise dimension remains more or less the same.

The topology of the mode OPD 3 in Fig. 5b is rather different, it is formed by two-roads of vortices in chequered pattern. The spacing is about ½ of that for the OPD 1. We remind, that this mode corresponds to the second harmonics Sr_2.

As the spacing of vortices is inversely proportional to the corresponding frequency, we could deduce that the convection velocity of the vortical patterns is more or less the same for all 3 OPD modes, around 70% of incoming velocity accelerating slowly downstream.

The higher OPD modes are characterized by relatively small periodicity p, this indicates that the appearance and disappearance of such modes is more random and short-time process. Theirs topologies are less regular, more random. We will show a few examples. The OPD 5 with relatively high frequency, $Sr = 0.52$, then OPD 6 with lower $Sr = 0.26$, even lower frequency $Sr = 0.16$ for OPD 7 and in the end the OPD 10 with $Sr = 0.08$. The real parts topologies of the above mentioned OPD modes are shown in Fig. 6a-d.

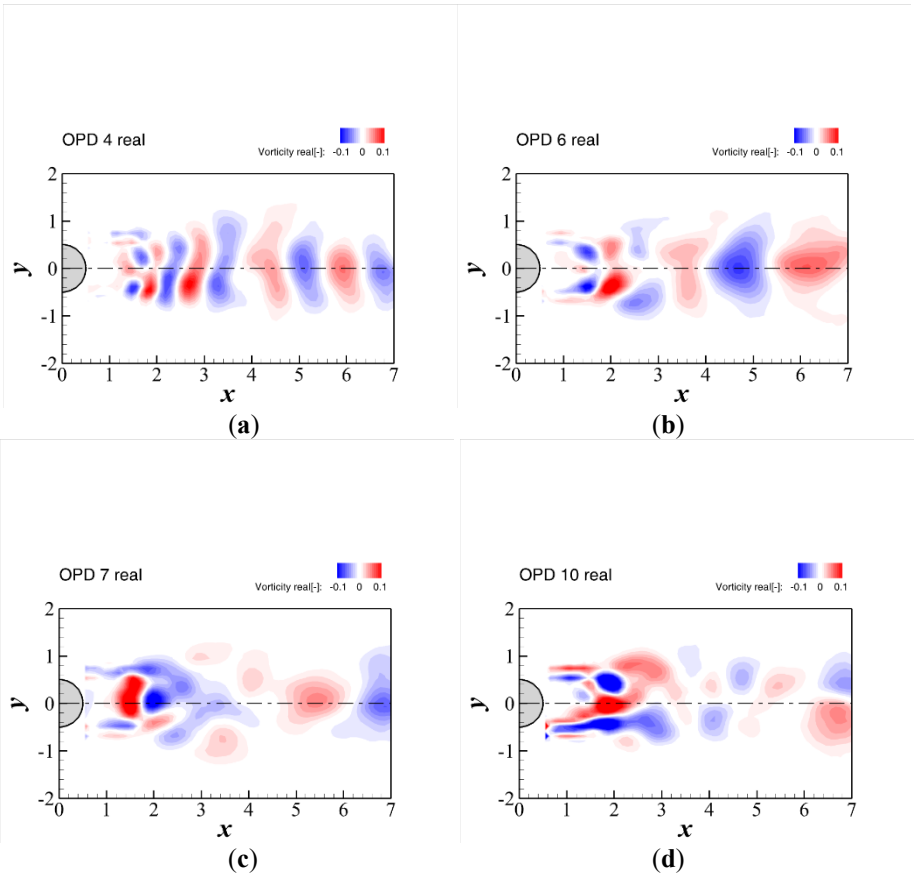

Fig. 6. OPD 4 (**a**), 6 (**b**),7 (**c**) and 10 (**d**) topologies, real parts.

The topologies of OPD modes in Fig. 6 are more pronounced in the near wake just behind the cylinder and they are linked to free shear layers in this region. The nature of dynamics is more pulsatile than wavy.

4 Conclusions

The circular cylinder turbulent wake is studied experimentally using Particle Image Velocimetry (PIV) method. The vorticity component parallel to the cylinder axis is evaluated from measured velocity field. Dynamics of the vorticity field is analysed using the Oscillation Pattern Decomposition (OPD) method.

The 3 dominant modes corresponding to the 1st, 2nd and 3rd harmonics of Strouhal frequency are detected and presented. The corresponding topologies are characterized by waves of vortical systems. The 1st and 3rd harmonic vortex waves are located on the x-axis in a single row, while the 2nd harmonic mode is represented by vortices in two-row chequered configuration. All vortex rows are convected in the streamwise direction, convection velocity is about 70 % of the incoming flow velocity in the near wake region accelerating gradually in the streamwise direction. Convection is more-or-less the same for all 3 modes.

The results obtained by the vorticity field analysis are similar to the dynamics of velocity field presented in [7], however the procedure is much easier to implement, as only half number of degrees of freedom are active.

This publication was supported by the project of University of West Bohemia in Pilsen SGS-2022-023.

References

1. von Kármán, T. (1954). Aerodynamics. *Columbus*: McGraw-Hill.
2. Roshko, A. (1955). On the development of turbulent wakes from vortex streets. *NACA Rep. 1191,* pp.801-825.
3. Williamson, C.H.K, (1996). Vortex Dynamics in the Cylinder Wake, *Annu. Rev. Fluid. Mech.* 28, pp. 477-539.
4. Uruba, V. (2016). On 3D instability of wake behind a cylinder, *AIP Conference Proceedings*, 1745, art. no. 020062.
5. Yanovych, V., Duda, D., Uruba, V. (2021). Structure turbulent flow behind a square cylinder with an angle of incidence, *European Journal of Mechanics, B/Fluids*, 85, pp. 110-123,
6. Duda, D., Uruba, V. (2019). Spatial Spectrum from Particle Image Velocimetry Data. *Journal of Nuclear Engineering and Radiation Science*, 5 (3), Article Number 030912
7. Uruba, V., and Procházka, P. (2020). On Harmonic Contents of the Wake behind a Circular Cylinder, *26th International Conference on Engineering Mechanics (IM), Engineering Mechanics 2020*, pp.500-503,
8. Uruba, V., Procházka, P., Skála, V. (2020). On the 3D Dynamics of the Wake Behind a Circular Cylinder, In *Proceedings Topical Problems of Fluid Mechanics 2020*, Prague, Edited by D. Šimurda and T. Bodnár, pp. 240-248,
9. Uruba, V. (2012). Decomposition methods in turbulent research, *EPJ Web of Conferences*, 25 01095.
10. Uruba, V. (2015). Near Wake Dynamics around a Vibrating Airfoil by Means of PIV and Oscillation Pattern Decomposition at Reynolds Number of 65 000, *Journal of Fluids and Structures*, 55, pp. 372-383.